Valley mixing in GaAs/AlAs multilayer structures in the effective-mass method

Y. Fu and M. Willander
Department of Physics and Measurement Technology, Linköping University, S-581 83 Linköping, Sweden

E. L. Ivchenko and A. A. Kiselev
A. F. Ioffe Physico-Technical Institute, Russian Academy of Sciences, 194021 St. Petersburg, Russia
(Received 16 November 1992)

We introduce a set of boundary conditions for electron envelope functions at GaAs/AlAs heterointerfaces so as to take into account Γ-X_z and X_x-X_y valley mixings in the effective-mass method. The proposed conditions enable one to obtain the dependence of the mixing effect upon the parity of monolayer numbers in AlAs and GaAs layers, in agreement with the empirical model calculations. The tunneling probability across a two-interface structure GaAs(AlAs)$_M$GaAs(001) is calculated as a function of the Γ-electron energy. The electron transfer is shown to depend essentially on the parity of M. An analytical solution is obtained for the dispersion of mixed X_{xy} minibands. Direct optical transitions are allowed between these minibands in the in-plane light polarization. The corresponding far-infrared absorption coefficient is calculated and estimated.

I. INTRODUCTION

GaAs/Al$_x$Ga$_{1-x}$As multilayer structures present convenient model systems for the study of valley-mixing effects associated with the superstructure potential (see, e.g., Refs. 1 and 2 and also references in Refs. 3 and 4 and in the review[5]). Since the mid 1980s different pseudopotential and tight-binding models[3–11] have been used for the calculation of GaAs/AlAs(001) superlattice (SL) minibands and for theoretical analysis of mixing between the Γ_1 conduction band and (001) X valley (Γ-X or Γ-X_z mixing) as well as between (100) and (010) X valleys (X_x-X_y mixing). The most striking common feature running through the results is a qualitative sensitivity of the valley-mixing effect on the parity of monolayer numbers in AlAs and GaAs layers. Ando and Akera[12] presented a generalized formulation of the effective-mass method in which Γ-X mixings at heterointerfaces are included by boundary conditions. However, in this formulation the parity of monolayer numbers has no influence on the miniband spectrum[12–14] in contrast with the results of the empirical model calculations. Aleiner and Ivchenko[15] showed that the boundary conditions of Ando and Akera are relevant to a single heteroboundary but they should be corrected in cases of double- or multiple-interface structures. If a factor changing its sign from one monolayer to another is introduced into the boundary conditions [see Eqs. (2.5) and (2.7) of the present paper], then the effective-mass approximation leads as well to the dependence of Γ-X mixing in a (GaAs)$_N$(AlAs)$_M$(001) SL on the parity of M.

In this work, we study tunneling properties of a GaAs(AlAs)$_M$GaAs single-barrier structure with an emphasis on the dependence whether the AlAs slab contains an even or odd number of monolayers (Sec. II). In Sec. III we propose a model effective-mass approximation to describe the X_x-X_y mixing, and in Sec. IV we analyze the lowest-lying X_{xy} minibands in a GaAs/AlAs SL and calculate the far-infrared (submillimeter) absorption coefficient under direct optical miniband transitions for the in-plane light polarization.

II. VALLEY MIXING BETWEEN Γ AND X_z

A. Three-band model

Figure 1 schematically shows the energy diagram of a GaAs/AlAs SL of the period $d=a+b$. In the following, the GaAs and AlAs layers are simply denoted by A and B, respectively. In the three-band model which takes into account mixing of Γ_1-band states with those from two close-lying bands X_1 and X_3, the electron wave function

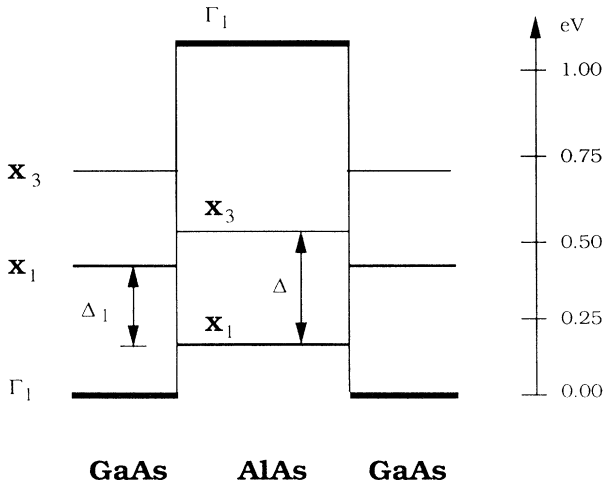

FIG. 1. The energy diagram of the GaAs/AlAs SL. Horizontal lines represent the edges of Γ_1, X_1, and X_3 bands in each bulk material.

is written as

$$\Psi_c(\mathbf{r})=w|\Gamma_1\rangle+v|X_3\rangle+u|X_1\rangle\ , \tag{2.1}$$

where $|\Gamma_1\rangle$, $|X_3\rangle$, and $|X_1\rangle$ are the Bloch functions of the corresponding symmetry at the Γ and X points. The effective Hamiltonian H is an operator on the envelopes $w(\mathbf{r})$, $v(\mathbf{r})$, and $u(\mathbf{r})$ and can be conveniently represented in the form of a 3×3 matrix,

$$H=\begin{vmatrix} H_\Gamma & \hat{V}_{\Gamma X} \\ \hat{V}_{X\Gamma} & \hat{H}_X \end{vmatrix}\ , \tag{2.2}$$

where the scalar H_Γ and 2×2 matrix $\hat{H}_X$ are Hamiltonians of Γ- and X-point electrons operating, respectively, on w and on the vector with two components v and u. In the effective-mass approximation we have

$$H_\Gamma=E_\Gamma^0(z)+\frac{\hbar^2}{2}\sum_\alpha \hat{k}_\alpha\frac{1}{m_\Gamma(z)}\hat{k}_\alpha\ , \tag{2.3}$$

$$\hat{H}_X=E_X^0(z)+\frac{\hbar^2k_z^2}{2m_X^{\parallel}}+\frac{\hbar^2k_\perp^2}{2m_X^{\perp}}+\frac{\Delta}{2}\hat{\sigma}_z+Rk_z\hat{\sigma}_y\ , \tag{2.4}$$

where $k_\alpha=-i\partial/\partial r_\alpha$ ($\alpha=x,y,z$), the Pauli matrices $\hat{\sigma}_y$ and $\hat{\sigma}_z$ are used to make the expression compact, $E_\Gamma^0(z)$ and $E_X^0(z)$ give positions of the Γ_1 minimum and the middle point between the X_1 and X_3 bands at the X point; they are constant inside each layer and discontinuous at the boundaries (Fig. 1); the effective mass of a Γ electron, $m_\Gamma(z)$, acquires the alternating values m_Γ^A and m_Γ^B in the GaAs and AlAs layers; Δ is the splitting between the X_1 and X_3 bands; the constant R describes the $\mathbf{k}\cdot\mathbf{p}$ interaction of these bands which leads to the camel-back structure of the X_1 conduction band. For simplicity we neglect the difference of $m_X^{\perp}$, $m_X^{\parallel}$, Δ, and R in adjacent layers. The off-diagonal operator $\hat{V}_{\Gamma X}=\hat{V}_{X\Gamma}^{+}$ is a 1×2 matrix describing the mixing of Γ and X states at heteroboundaries. Its form depends on boundary conditions imposed upon the envelope functions. We assume the envelopes w, v, and u to be continuous at heterointerfaces and use the boundary conditions for derivatives in the form proposed by Ando and Akera[12] and improved by Aleiner and Ivchenko,[15]

$$\nabla_X v_A=\nabla_x v_B+t_{\Gamma X}^{(1)}w_B\ , \tag{2.5a}$$

$$\nabla_\Gamma^A w_A=\nabla_\Gamma^B w_B+t_{\Gamma X}^{(2)}v_B\ , \tag{2.5b}$$

$$\nabla_X u_A=\nabla_X u_B\ . \tag{2.5c}$$

Here

$$\nabla_X=a_0\frac{m_0}{m_X^{\parallel}}\frac{\partial}{\partial z}\ ,\quad \nabla_\Gamma^f=a_0\frac{m_0}{m_\Gamma^f}\frac{\partial}{\partial z}\ , \tag{2.6}$$

a_0 is the lattice constant (in GaAs, $a_0=5.6$ Å), m_0 is the free-electron mass, $f=A,B$. By using the dimensionless derivatives (2.6), one can introduce the dimensionless coefficients $t_{\Gamma X}^{(j)}$ ($j=1,2$) as a measure of the Γ-X mixing strength. From the requirement of electron flux continuity at a heteroboundary one obtains the relation $t_{\Gamma X}^{(2)}=t_{\Gamma X}^{(1)*}$. According to the empirical tight-binding-model calculation[12] performed for a single GaAs/$Al_xGa_{1-x}As$ heterojunction, $t_{\Gamma X}^{(1)}$ and $t_{\Gamma X}^{(2)}$ are real and can be estimated by $t_{\Gamma X}^{(1)}=qx$ with $q\approx1$, x being the Al concentration in the barriers.

The coefficients $t_{\Gamma X}^{(j)}$ were considered in Refs. 12–14 to be independent of the coordinate, z_{if}, of a heteroboundary between layers. In this case the miniband spectrum obtained in the effective-mass approximation is determined by the layer thicknesses a and b, whereas the parity of AlAs monolayer number in a B layer does not play a role of an additional parameter in contradiction with the results of empirical model calculations. In fact, the coefficients $t_{\Gamma X}^{(j)}$ in Eq. (2.5) should be written in the form

$$t_{\Gamma X}^{(1)}(z_{if})=t_{\Gamma X}^{(2)}(z_{if})=t_{\Gamma X}\eta(z_{if})\ , \tag{2.7}$$

where the phase factor $\eta(z_{if})=\exp(2\pi iz_{if}/a_0)=\cos(2\pi z_{if}/a_0)$ takes the two values ±1 varying from one to another monolayer. The presence of the factor $\eta(z_{if})$ in Eq. (2.7) can be understood taking into account that under translation by the basic vector $\mathbf{a}_2=(a_0/2)(0,1,1)$ or $\mathbf{a}_3=(a_0/2)(1,0,1)$ (which corresponds to a shift along the principal axis z by a single monomolecular layer), the electron function $|\Gamma_1\rangle$ remains unchanged while Bloch functions at the point $\mathbf{k}_x=(2\pi/a_0)(0,0,1)$ change their sign. Note that for a single heteroboundary the sign of η can be chosen arbitrarily since the corresponding phase change can be introduced into the envelope w or into the envelopes v, u. However, this choice unambiguously fixes the phase $\Phi=2\pi z_{if}/a_0$ at any other heteroboundary of the same structure.

The additional terms on the right-hand side of Eq. (2.5) are equivalent to inclusion into the effective Hamiltonian (2.2) of the operator $\hat{V}_{\Gamma X}=(V_{\Gamma_1X_3},V_{\Gamma_1X_1})$ with $V_{\Gamma_1X_1}=0$ and

$$V_{\Gamma_1X_3}=\sum_l a_0U\eta(z_l)\zeta_l\delta(z-z_l)\ , \tag{2.8}$$

where $U=\hbar^2t_{\Gamma X}/(2a_0^2m_0)$, z_l is the heteroboundary coordinate, $\zeta_l=1$ for the boundary AlAs/GaAs, and $\zeta_l=-1$ for the boundary GaAs/AlAs. The factor ζ_l arises in Eq. (2.8) because the operator $\partial/\partial z$ is antisymmetric under the coordinate change $z\to-z$ (see Ref. 13). Now the Hamiltonian (2.2) is completely defined and can be used for the miniband spectra calculation.

In order to demonstrate the role of the phase factors $\eta(z_l)$ it is instructive to calculate the energy dispersion for the two lowest electron minibands in $(GaAs)_N(AlAs)_M$ SL's near the transition from type I to type II. (The boundary between type-I and type-II GaAs/AlAs SL's was analyzed experimentally in Refs. 16 and 17.) In this case one can first calculate the lowest minibands $e1\Gamma$ and $e1X$ for Γ and X_z minima in the absence of the Γ-X mixing and then include the interaction (2.8) between them. In the effective-mass tight-binding approximation, one obtains the following dispersion curves:[15]

$$E_{\pm}(\mathbf{k})=\tfrac{1}{2}(E_{\Gamma}(\mathbf{k})+E_X(\mathbf{k}) \pm\{[E_{\Gamma}(\mathbf{k})-E_X(\mathbf{k})]^2+16\bar{V}^2\chi\}^{1/2}) \quad (2.9)$$

with the energies for unmixed Γ- and X_z-point states given by

$$E_{\Gamma}(\mathbf{k})=\bar{E}_{\Gamma}+\frac{J}{2}(1-\cos k_z d)+\frac{\hbar^2 k_{\perp}^2}{2M_{\Gamma}^{\perp}} , \quad (2.10a)$$

$$E_X(\mathbf{k})=\bar{E}_X+\frac{\hbar^2 k_{\perp}^2}{2M_X^{\perp}} . \quad (2.10b)$$

Here $\bar{E}_{\mu}$ is the electron energy in a single-quantum-well structure AlAs/GaAs/AlAs ($\mu=\Gamma$) or GaAs/AlAs/GaAs ($\mu=X$), $M_{\mu}^{\perp}$ is the corresponding effective mass for the electron movement in the (x,y) plane and slightly differs from m_A^{Γ} and $m_X^{\perp}$, J is the overlap integral connected with the $e1\Gamma$-miniband-bottom effective mass $M_{\perp}^{\parallel}=2\hbar^2/Jd$. Other notations introduced in Eq. (2.9) are

$$\bar{V}=a_0 U w^0(BA)v^0(BA) , \quad (2.11)$$

$$\chi=\cos^2(k_z d/2+\bar{\Phi}) , \quad \bar{\Phi}=M\pi/2 , \quad (2.12)$$

$w^0(z)$ is the envelope function for a Γ electron in a GaAs single quantum well of the width a, v^0 and u^0 are the envelopes for an X electron in an AlAs single quantum well of the width b, M is the AlAs monolayer number in a B layer, $d=a+b$ is the SL period, and the symbol BA means a coordinate of the heteroboundary AlAs/GaAs. The parity of AlAs monolayer number is explicitly present in the expression (2.12), and hence in the dispersion (2.9). When M is even, the phase $\bar{\Phi}$ is an integer number of π, $\chi=\cos^2(k_z d/2)$, and the states $e1\Gamma$, $e1X$ are mixed at $k_z=0$ and do not mix at $k_z=\pi/d$. On the contrary, in the case of odd M, $\chi=\sin^2(k_z d/2)$, the ΓX mixing is allowed at the SL Brillouin zone boundary while at $k_z=0$ the mixing is absent.

The existence or absence of the ΓX mixing between the $e1\Gamma$ and $e1X$ states at $k_z=0$ and $k_z=\pi/d$ can be understood in terms of the general group-theoretical approach.[3-5] While making the symmetry analysis, one should take into account that, in bulk GaAs or AlAs, the X_1 state is invariant under mirror rotation S_{4z}(As) relative to an origin on an anion site and antisymmetric under the transformation S_{4z}(Ga) with an origin on a cation site. The parity of the X_3 state is opposite to that of the X_1 state. As far as the Γ_1 Bloch function is concerned, it is invariant with respect to both S_{4z}(As) and S_{4z}(Ga) transformations. The space structure of $(GaAs)_N(AlAs)_M$ SL's is characterized by the D_{2d} point-group symmetry which comprises the transformation S_{4z} with the origin at the midpoint in an AlAs (or GaAs) slab. For the lowest minibands $e1\Gamma$ and $e1X$ the parity of states $k_z=0$ with respect to this transformation coincides with that of the Bloch functions $|\Gamma_1\rangle$ and $|X_1\rangle$. This readily follows from a simple consideration in the Kronig-Penney model for Γ and X electrons neglecting the ΓX mixing. For even M, the central atomic plane in an AlAs slab is occupied by As atoms and, therefore, the states $e1\Gamma$, $e1X$ at $k_z=0$ have the same symmetry and they can mix in an ideal SL in agreement with Eq. (2.12). For odd M, the central plane is occupied by Al atoms which means that the states $e1\Gamma$, $e1X$ differ in symmetry and will mix only by interface imperfections.[4] The symmetry analysis of the states at $k_z=\pi/d$ is carried out in a similar fashion. It is worth mentioning that in the case of reversed energy positions of X_1 and X_3 states, i.e., for the lowest X-point conduction band being X_3, the cosine in Eq. (2.12) would be replaced by sine.

B. Transmission probability calculations

A double-interface structure $GaAs(AlAs)_M GaAs$ is used to study the effect of the Γ-X mixing on the transmission probability as a function of incident electron energy. Throughout this paper, the structure growth direction is chosen as the z direction. Band parameters used in the calculations are listed in Table I. We assume $t_{\Gamma X}=1$ in which case $t_{\Gamma X}^{(j)}=t_{\Gamma X}\eta(z_{if})=\eta(z_{if})$ [see Eq. (2.7)]. The phase $\Phi=2\pi z/a_0$ at the left interface ($z=0$) is set to zero so that $t\equiv t_{\Gamma X}^{(j)}(z=0)=1$. The right interface is at $z=Ma_0/2$. Three situations are discussed.

(a) For odd M, $t'\equiv t_{\Gamma X}^{(j)}(Ma_0/2)=-1$ due to the phase-dependent factor η in Eq. (2.7). We call this case FWIK.

(b) For odd M we set $t'=1$ neglecting the factor η, the AA case, which was used by Ando and Akera[12] (see also Refs. 13 and 14).

(c) For even M, $t'=t=1$.

Numerical results are presented in Figs. 2 and 3. For a Γ electron, the AlAs layer is the potential barrier, whereas it is the GaAs layer that plays a role of barrier for an X electron. So in the $GaAs(AlAs)_M GaAs$ system, subbands are formed for the X electrons. When the energy E of the incident Γ electron is matched with one of the X subbands, the Γ electron is assisted to tunnel through the AlAs Γ barrier due to the Γ-X mixing. This explains the peaks in the transmission probability which otherwise increases monotonously with increasing Γ electron energy. Numerical calculation shows that the positions of peaks in the transmission probability spectra mark exactly the X subbands.

For further understanding of Figs. 2 and 3, analytical

TABLE I. Parameters used in calculations. $R=[(\hbar^2/m_X^{\parallel})P]^{1/2}$, $P=Y_m+(Y_m^2+\Delta^2/4)^{1/2}$, $Y_m=\hbar^2 k_m^2/2m_X^{\parallel}$. In calculations, the averaged values of R, Δ, and $m_X^{\parallel}$ are used.

	GaAs	AlAs
E_X^0 (eV)	0.5645[a]	0.3424[a]
E_{Γ}^0 (eV)	0.0[a]	1.1094[a]
Δ (eV)	0.304[b]	0.350[b]
k_m	$0.102(2\pi/a_0)$[b]	$0.097(2\pi/a_0)$[b]
R (eV Å)	0.876	1.004
m_{Γ} (m_0)	0.067[b]	0.150[b]
$m_X^{\parallel}$ (m_0)	1.800[b]	1.560[b]

[a]Reference 13.
[b]Reference 18.

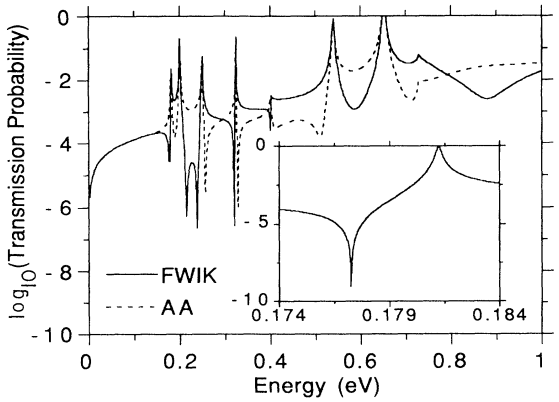

FIG. 2. Tunneling probabilities as a function of the electron energy across a single-barrier structure $GaAs(AlAs)_9GaAs$ calculated neglecting (AA) and taking into account (FWIK) the phase factors $\eta(z_{if})$ in the boundary conditions (2.5), (2.7).

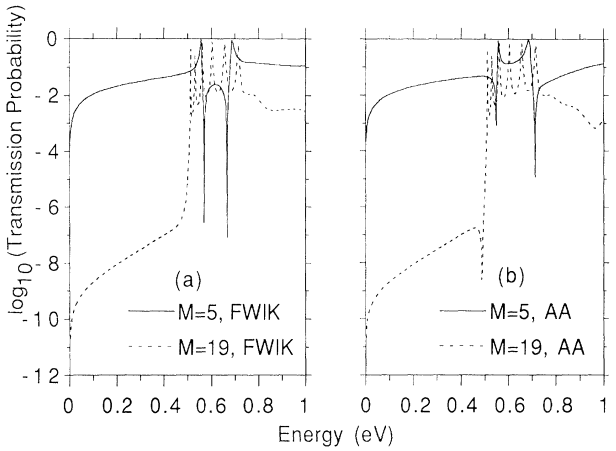

FIG. 4. Transmission probability in the absence of $\mathbf{k}\cdot\mathbf{p}$ interaction between X_1 and X_3 bands ($R=0$). $M=5$, 19. (a) FWIK. (b) AA.

analysis is discussed in the simplified case of $R=0$. When $R=0$, only the Γ_1 and X_3 states are mixed, which is demonstrated in Fig. 4. Since the Γ-X mixing happens at interfaces, the Γ_1 and X_3 states propagate independently both in GaAs and in AlAs layers. Let us discuss the situation when the energy of the incident Γ electron is below the X_3(GaAs), since it is the most transparent for analysis. The incoming Γ electron with the energy E at $z=0^-$ is characterized by the plane wave e^{ikz}, where $\hbar k=(2m_\Gamma^A E)^{1/2}$; the reflected and transmitted Γ electrons are, respectively, re^{-ikz} ($z<0$) and $Te^{ik(z-b)}$ ($z>b$, $Ma_0/2=b$). Due to the Γ-X mixing, X_3 states, ρe^{sz} when $z<0$ and $\tau e^{-s(z-b)}$ when $z>b$, are expected as well, where $\hbar s=\{2m_X^{\downarrow}[E_{X_3}(\mathrm{GaAs})-E]\}^{1/2}$.

Let $\hbar g=\{2m_\Gamma[E_\Gamma(\mathrm{AlAs})-E]\}^{1/2}$, $\hbar q=\{2m_X^{\downarrow}[E-E_{X_3}(\mathrm{AlAs})]\}^{1/2}$, $\lambda_\Gamma^A=a_0(m_0/m_\Gamma^A)k$, $\lambda_\Gamma^B=a_0(m_0/m_\Gamma^B)g$, $\eta_X^A=a_0(m_0/m_X^{\downarrow})s$, and $\eta_X^B=a_0(m_0/m_X^{\downarrow})q$. By the matching conditions of Eq. (2.5) and the proper consideration of the wave propagation in the AlAs layer, we have the following matrix equation:

$$\begin{bmatrix} 1+r \\ i\lambda_\Gamma^A(1-r) \\ \rho \\ \eta_x^A\rho \end{bmatrix} = \hat{T}_{AB}\hat{T}_{BB}\hat{T}_{BA}\begin{bmatrix} T \\ i\lambda_\Gamma^A T \\ \tau \\ -\eta_X^A\tau \end{bmatrix} . \tag{2.13}$$

Here the transfer matrix $\hat{T}_{ff'}$ connects the four-component vector

$$\left[w, a_0\frac{m_0}{m_\Gamma}\frac{dw}{dz}, v, a_0\frac{m_0}{m_X^{\downarrow}}\frac{dv}{dz}\right]$$

at the left- and right-hand sides of the interface AlAs/GaAs ($\hat{T}_{BA}$) and GaAs/AlAs ($\hat{T}_{AB}$) or at the opposite boundaries of the AlAs layer ($\hat{T}_{BB}$). The matrix $\hat{T}_{BB}$ is quasidiagonal,

$$\hat{T}_{BB}=\begin{bmatrix} \hat{\Gamma} & 0 \\ 0 & \hat{X} \end{bmatrix} , \tag{2.14a}$$

where the transfer matrices for Γ and X electrons are given by

$$\hat{\Gamma}=\begin{bmatrix} \Gamma_{11} & \Gamma_{12} \\ \Gamma_{21} & \Gamma_{22} \end{bmatrix} = \begin{bmatrix} \cos(gb) & -\frac{1}{\lambda_\Gamma^B}\sinh(gb) \\ -\lambda_\Gamma^B\sinh(gb) & \cosh(gb) \end{bmatrix} , \tag{2.14b}$$

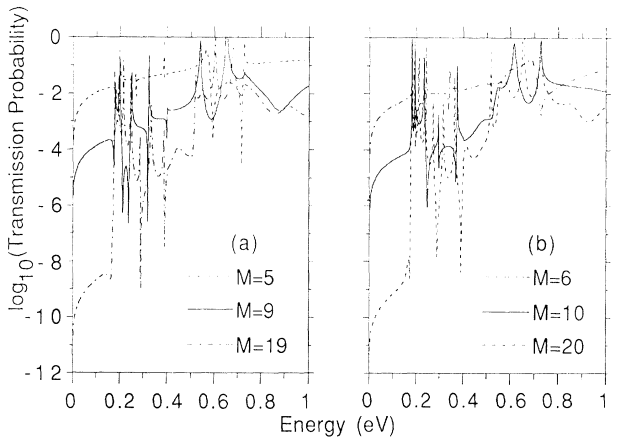

FIG. 3. Tunneling probabilities as a function of energy across a single-barrier structure $GaAs(AlAs)_MGaAs$ for different monolayer numbers M. The phase factors $\eta(z_{if})$ are taken into account in the calculations. (a) $M=5$, 9, 19. (b) $M=6$, 10, 20.

$$\hat{X}=\begin{bmatrix} X_{11} & X_{12} \\ X_{21} & X_{22} \end{bmatrix}=\begin{bmatrix} \cos(qb) & -\dfrac{1}{\eta_X^B}\sin(qb) \\ \eta_X^B\sin(qb) & \cos(qb) \end{bmatrix} . \tag{2.14c}$$

Taking into account the boundary conditions (2.5) we obtain for the interface transfer matrices

$$\hat{T}_{AB}=\begin{bmatrix} 1 & 0 & 0 & 0 \\ 0 & 1 & t & 0 \\ 0 & 0 & 1 & 0 \\ t & 0 & 0 & 1 \end{bmatrix} , \quad \hat{T}_{BA}=\begin{bmatrix} 1 & 0 & 0 & 0 \\ 0 & 1 & -t' & 0 \\ 0 & 0 & 1 & 0 \\ -t' & 0 & 0 & 1 \end{bmatrix} . \tag{2.15}$$

The solution of Eq. (2.13) for the transmission amplitude coefficient T can be written as

$$T=\frac{2i\lambda_\Gamma^A(\Sigma_X-tt'\Gamma_{12})}{\Sigma_X\Sigma_\Gamma-2t^2(X_{11}-\eta_x^A X_{12})(\Gamma_{11}+i\lambda_\Gamma^A\Gamma_{12})+t^4X_{12}\Gamma_{12}+2tt'} , \tag{2.16}$$

where we use the notations $\Sigma_\Gamma=\Gamma_{21}-(\lambda_\Gamma^A)^2\Gamma_{12}+2i\lambda_\Gamma^A\Gamma_{11}$ and $\Sigma_X=X_{21}+(\eta_x^A)^2X_{12}-2\eta_X^AX_{11}$ and take into account the identity $t^2=(t')^2$. Note that the solutions of the equation $\Sigma_X=0$ give the quantum-confinement energy states of an X electron for the GaAs(AlAs)$_M$GaAs structure in the absence of Γ-X mixing.

When E is close to a subband E_{evX}, Σ_X can be approximated by the linear dependence $P_v(E-E_{evX})$, the coefficient P_1 of the lowest subband being positive since $\Sigma_X<0$ in the region $0<E<E_{e1X}$. According to Eq. (2.14a) the component Γ_{12} is negative. Then, for $t=t'$, the factor $(\Sigma_X-tt'\Gamma_{12})$ in the denominator of Eq. (2.16) vanishes at some point $E<E_{e1X}$ while, in the case $t'=-t$, the denominator has no zeros in this region in agreement with Fig. 4. The last term in the denominator is proportional to the product tt' and independent on the $\hat{\Gamma}$-matrix components. This means that for barriers thick enough so that $\exp(gb)\gg1$, this term can be ignored and the peak positions given by the denominator minimum become the same for $t'=1$ and $t'=-t$.

III. VALLEY MIXING BETWEEN X_x AND X_y

Here we extend the Kronig-Penney model to reproduce the X_x-X_y mixing in a similar fashion as it was made in the preceding section for the Γ-X_z mixing.

A. Boundary conditions

Let us introduce the envelope functions u_x, u_y, v_x, and v_y which describe admixture of $|X_{1x}\rangle$, $|X_{1y}\rangle$, $|X_{3x}\rangle$, and $|X_{3y}\rangle$ states in the electron wave function. We propose the following boundary conditions for this set of envelopes at interfaces AB or BA.

For both AB and BA interfaces:

$$\begin{aligned} &u_x^A=u_x^B , \quad u_y^A=u_y^B , \\ &v_x^A=v_x^B , \quad v_y^A=v_y^B . \end{aligned} \tag{3.1}$$

For AB (GaAs/AlAs) interfaces:

$$\begin{aligned} &\nabla_x^\perp u_\alpha^A=\nabla_x^\perp u_\alpha^B+t_{xy}^{(u)}\eta(z_{if})u_\beta^B , \\ &\nabla_x^\perp v_\alpha^A=\nabla_y^\perp v_\alpha^B+t_{xy}^{(v)}\eta(z_{if})v_\beta^B . \end{aligned} \tag{3.2a}$$

For BA (AlAs/GaAs) interfaces:

$$\begin{aligned} &\nabla_x^\perp u_\alpha^A=\nabla_x^\perp u_\alpha^B-t_{xy}^{(u)}\eta(z_{if})u_\beta^B , \\ &\nabla_x^\perp v_\alpha^A=\nabla_x^\perp v_\alpha^B-t_{xy}^{(v)}\eta(z_{if})v_\beta^B . \end{aligned} \tag{3.2b}$$

Here superscripts A and B denote interface boundaries z_{if} from the side of GaAs and AlAs, respectively,

$$\nabla_x^\perp=a_0\frac{m_0}{m_X^\perp}\frac{\partial}{\partial z} , \tag{3.3}$$

$t_{xy}^{(u)}$, $t_{xy}^{(v)}$ are real dimensionless constants, $\alpha=x,y$, $\beta=y$ if $\alpha=x$ and $\beta=x$ if $\alpha=y$, and $\eta(z_{if})$ is the phase factor $\exp(2\pi iz_{if}/a_0)=\cos(2\pi iz_{if}/a_0)$ as in Eq. (2.7). The opposite signs of the terms in Eqs. (3.2a) and Eqs. (3.2b) describing the X_x-X_y mixing are connected with the antisymmetric nature of the operator $\partial/\partial z$ under transformation S_{4z} changing z to $-z$, u_x to u_y and u_y to u_x. The presence of the factor η in Eqs. (3.2) can be understood taking into account that for a bulk zinc-blende structure there exists the reciprocal-lattice vector $\mathbf{b}=(2\pi/a_0)(1,-1,1)$. The superstructural potential removes the wave-vector conservation along the z direction and allows mixing between states with $\mathbf{k}$'s differing by the vector $(2\pi/a_0)(1,-1,0)$. However, the memory about the nonzero z component $b_z=2\pi/a_0$ should be retained in those terms in the boundary conditions that determine the state mixing. Note that Eqs. (3.1) and (3.2) are the simplest boundary conditions for the envelopes $u_{x,y}$, $v_{x,y}$ which are allowed by symmetry, maintain continuity of the electron flux at interfaces, and take into account the X_x-X_y mixing effect. Similar to Sec. II A [see Eq. (2.8)], the inclusion of extra terms in Eqs. (3.2) is equivalent to an additional δ-functional perturbation potential. In the basis X_{1x}, X_{1y}, X_{3x}, and X_{3y}, the potential has the following 4×4 matrix form:

$$\hat{V}_{xy}=\sum_l a_0\eta(z_l)\delta(z-z_l)\begin{vmatrix} U^{(u)}\hat{I} & 0 \\ 0 & U^{(v)}\hat{I}\end{vmatrix}, \tag{3.4}$$

where $U^{(u,v)}=-\hbar^2 t_{xy}^{(u,v)}/2a_0^2 m_0$, $\hat{I}$ is the unit 2×2 matrix.

B. Subbands along $(a^*, 0, fc^*)$

First, we consider the states in a $(GaAs)_N(AlAs)_M$ SL with wave vectors $(a^*,0,fc^*)$, where $a^*=2\pi/a_0$, $c^*=2\pi/[a_0(N+M)]$, $0\le|f|\le 1$. A more general case of the wave vector (a^*+k_x,k_y,fc^*) will be considered in the next section. If $k_x=k_y=0$, then the states X_1 and X_3 are not coupled and can be analyzed independently. We concentrate here on the analysis of the lowest X_{1x} and X_{1y} states.

In the absence of X_x-X_y mixing we have two degenerate states

$$\Psi_{ak_z}(z)=\frac{1}{\sqrt{\mathbf{N}}}\sum_m e^{ik_z dm}u_\alpha^0(z-dm). \tag{3.5}$$

Here $\alpha=x$ and y, k_z coincides with fc^*, and $\mathbf{N}$ is the number of SL periods. As in Ref. 15, we use the tight-binding approximation in order to take into account the tunneling of an electron along the z direction so that u_α^0 are the X-electron envelope functions in a single-quantum-well structure GaAs/AlAs/GaAs.

For the states $e1X$, $e3X$, . . . ,

$$u_\alpha^0(z)\equiv u^0(z)=\begin{cases} C\cos(qz) & \text{if } |z|\le b/2 \\ C\cos(qb/2)e^{-s(|z|-b/2)} & \text{if } |z|\ge b/2\end{cases}, \tag{3.6a}$$

and for the states $e2X$, $e4X$, . . . ,

$$u^0(z)=\begin{cases} D\sin(qz) & \text{if } |z|\le b/2 \\ D\sin(qb/2)\mathrm{sgn}(z)e^{-s(|z|-b/2)} & \text{if } |z|\ge b/2\end{cases}, \tag{3.6b}$$

where $q=(2m_X^{\perp}E/\hbar^2)^{1/2}$, $s=[2m_X^{\perp}(\Delta_1-E)/\hbar^2]^{1/2}$, E is the electron energy referred to the energy $E(X_1)$ at the X point, and Δ_1 is the X_1-band offset (see Fig. 1). The normalization coefficients C and D are found from the relation

$$\int_{-\infty}^{+\infty}dz|u^0(z)|^2=1. \tag{3.7}$$

1. Interaction between Ψ_{xk_z} and Ψ_{yk_z}

By using Eqs. (3.4) and (3.5), one can obtain for the matrix element of the X_x-X_y mixing,

$$V_{xy}\equiv\langle X_x,k_z|\hat{V}_{xy}|X_y,k_z\rangle = a_0U^{(u)}[u^0(BA)]^2(e^{iM\pi/2}+e^{-iM\pi/2})\frac{1}{\mathbf{N}}\sum_m e^{im(N+M)\pi}, \tag{3.8}$$

where m labels the superlattice unit cells in the z direction. We took into account that, at interfaces $z_m^{\pm}=dm\pm b/2$ of the mth AlAs layer, the phase factor can be rewritten as

$$\eta(z_m^{\pm})=e^{im(N+M)\pi/2}e^{\pm iM\pi/2},$$

because $d=a_0(N+M)/2$ and $b=Ma_0/2$. If M is odd, then the sum of the two exponents $\exp(\pm iM\pi/2)$ is zero and the matrix element (3.8) vanishes. On the other hand, if M is even, then

$$e^{iM\pi/2}+e^{-iM\pi/2}=\pm 2. \tag{3.9}$$

As far as the sum over m in Eq. (3.8) is considered it can be written as

$$\frac{1}{\mathbf{N}}\sum_m e^{im(N+M)\pi}=\begin{cases}1 & \text{for even } N+M \\ 0 & \text{for odd } N+M\end{cases}. \tag{3.10}$$

It follows then that the states Ψ_{xk_z} and Ψ_{yk_z} will mix only if both N and M are even, in which case the splitting between the mixed states $(1/\sqrt{2})(\Psi_{xk_z}\pm\Psi_{yk_z})$ is

$$\Delta_{xy}=4a_0|U^{(u)}|[u^0(BA)]^2. \tag{3.11}$$

From a comparison with the results of the numerical calculation[3] one can extract $U^{(u)}$, and hence obtain an estimation for $t_{xy}^{(u)}$.

2. Interaction between Ψ_{xk_z} and Ψ_{y,k_z-c^*}

Calculating the matrix element of the operator (3.4) between the states Ψ_{xk_z} and Ψ_{y,k_z-c^*}, one obtains

$$V'_{xy}\equiv\langle X_x,k_z|\hat{V}_{xy}|X_y,k_z-c^*\rangle = a_0U^{(u)}[u^0(BA)]^2(e^{iM\pi/2}+e^{-iM\pi/2})\times\frac{1}{\mathbf{N}}\sum_m e^{-ic^*dm}e^{im(N+M)\pi}. \tag{3.12}$$

For odd M this matrix element vanishes as well as V_{xy} in Eq. (3.8). Taking into account that $c^*d=\pi$ and

$$e^{im(N+M)\pi}=\begin{cases}1 & \text{for even } N+M \\ e^{im\pi} & \text{for odd } N+M\end{cases}, \tag{3.13}$$

one can easily transform Eq. (3.12) to

$$V'_{xy}=\pm 2a_0U^{(u)}[u^0(BA)]^2\times\begin{cases}1 & \text{if } N \text{ odd and } M \text{ even} \\ 0 & \text{if either } N \text{ even or } M \text{ odd}\end{cases}. \tag{3.14}$$

3. Brief summary

Thus, the results for the four possible cases can be summarized as follows.

Case I. N and M both even,

$$E^{\pm}(k_z)=\bar{E}_X+\frac{J_{\perp}}{2}[1-\cos(k_zd)]\pm|V_{xy}|. \tag{3.15a}$$

Case II. N and M both odd,

$$E^{\pm}(k_z)=\bar{E}_X+\frac{J_\perp}{2}[1-\cos(k_z d)] . \tag{3.15b}$$

Case III. N and odd and M even,

$$E^{\pm}(k_z)=\bar{E}_X+\frac{J_\perp}{2}\pm\left[(V'_{xy})^2+\left[\frac{J_\perp}{2}\cos(k_z d)\right]^2\right]^{1/2} . \tag{3.15c}$$

Case IV. N even and M odd,

$$E^{\pm}(k_z)=\bar{E}_X+\frac{J_\perp}{2}[1\pm\cos(k_z d)] . \tag{3.15d}$$

$J_\perp$ is the overlap integral dependent on the effective mass $m_x^\perp$. In case III we took into account that $\cos[(k_z-c^*)d]=-\cos(k_z d)$. It is seen from Eq. (3.15d) that in the tight-binding approximation the state splitting at $k_z=c^*/2$ is zero. The analytical results presented by Eqs. (3.15a)–(3.15d) are in a complete agreement with those obtained numerically by Lu and Sham (see Fig. 10 of Ref. 3).

C. Symmetry conditions

One can show that in a bulk GaAs the twofold rotations C_{2x}(Ga) and C_{2x}(As) are interconnected by

$$C_{2x}(\mathrm{Ga})=t_{\mathbf{a}_2}C_{2x}(\mathrm{As}) , \tag{3.16a}$$

while for the twofold rotations around the y axis one has

$$C_{2y}(\mathrm{Ga})=t_{\mathbf{a}_3}C_{2y}(\mathrm{As}) , \tag{3.16b}$$

where $\mathbf{a}_2=\frac{1}{2}a_0(0,1,1)$ and $\mathbf{a}_3=\frac{1}{2}a_0(1,0,1)$. From Eqs. (3.16) the following symmetry properties of the states $|X_{1x}\rangle$ and $|X_{1y}\rangle$ are derived:

$$\begin{aligned} &C_{2\alpha}(\mathrm{As})|X_{1\beta}\rangle=|X_{1\beta}\rangle \quad (\alpha,\beta=x,y) , \\ &C_{2\alpha}(\mathrm{Ga})|X_{1\alpha}\rangle=|X_{1\alpha}\rangle \quad (\alpha\neq\beta) , \\ &C_{2\alpha}(\mathrm{Ga})|X_{1\beta}\rangle=-|X_{1\beta}\rangle \quad (\alpha\neq\beta) . \end{aligned} \tag{3.17}$$

While deriving Eq. (3.17) we used the translational properties of Bloch functions at the X_x and X_y points:

$$\begin{aligned} &t_{\mathbf{a}_2}|X_{1x}\rangle=|X_{1x}\rangle , \quad t_{\mathbf{a}_2}|X_{1y}\rangle=-|X_{1y}\rangle , \\ &t_{\mathbf{a}_3}|X_{1x}\rangle=-|X_{1x}\rangle , \quad t_{\mathbf{a}_3}|X_{1y}\rangle=|X_{1y}\rangle . \end{aligned} \tag{3.18}$$

Thus, for either N or M odd, when the central plane of a GaAs or AlAs layer is occupied by cation atoms the states $|X_{1x}\rangle$ and $|X_{1y}\rangle$ differ in symmetry and will not mix if the corresponding envelope functions u_x and u_y are characterized by the same symmetry. For N and M both even the central planes of the GaAs and AlAs layers are occupied by anion atoms and the symmetries of the states $|X_{1x}\rangle$ and $|X_{1y}\rangle$ states coincide, which means that they can mix.

It is instructive to reiterate that the basis vectors of the reciprocal lattice corresponding to $(\mathrm{GaAs})_N(\mathrm{AlAs})_M$ SL's are (see, e.g., Ref. 3) for $N+M$ even,

$$\begin{aligned} &\mathbf{a}_1^*=a^*(1,1,0) , \\ &\mathbf{a}_2^*=a^*(-1,1,0) , \\ &\mathbf{a}_3^*=2c^*(0,0,1) , \end{aligned} \tag{3.19a}$$

and for $N+M$ odd,

$$\begin{aligned} &\mathbf{a}_1^*=(a^*,a^*,-c^*) , \\ &\mathbf{a}_2^*=(-a^*,a^*,-c^*) , \\ &\mathbf{a}_3^*=2c^*(0,0,1) . \end{aligned} \tag{3.19b}$$

Since the difference between the wave vectors $\mathbf{K}_2=(0,a^*,-(1-f)c^*)$ and $\mathbf{K}_1=(a^*,0,fc^*)$ is $(-a^*,a^*,-c^*)$, which is nothing more than $\mathbf{a}_2^*$ in Eq. (3.19b), $\mathbf{K}_1$ and $\mathbf{K}_2$ are equivalent vectors and the corresponding states are allowed to be mixed in an ideal SL in accordance with the above-considered case III. The above symmetry analysis is completely valid for the mixing between the states with

$$\mathbf{K}_1=(a^*+k_x,k_y,fc^*) , \quad \mathbf{K}_2=(k_x,a^*+k_y,-(1-f)c^*) .$$

IV. X_x AND X_y MIXING. DEPENDENCE ON k_x, k_y

A. The energy dispersion

For $k_{x,y}\neq 0$, the X-valley states X_1 and X_3 are coupled and should be treated together. If we use a four-component envelope function

$$\Psi=\begin{bmatrix} v_x \\ u_x \\ v_y \\ u_y \end{bmatrix} \tag{4.1}$$

to represent the electronic state in a SL, the electronic Hamiltonian can be written as

$$H=\begin{bmatrix} \hat{H}_x & \hat{V}_{xy} \\ \hat{V}_{xy} & \hat{H}_y \end{bmatrix} , \tag{4.2}$$

where

$$\begin{aligned} \hat{H}_x&=\frac{\Delta}{2}\hat{\sigma}_z+Rk_x\hat{\sigma}_y+E_{e1X}^{\perp} \\ &\quad+\frac{J_\perp}{2}[1-\cos(k_z d)]+\frac{\hbar^2k_x^2}{2m_X^{\parallel}}+\frac{\hbar^2k_y^2}{2m_X^{\perp}} , \\ \hat{H}_y&=\frac{\Delta}{2}\hat{\sigma}_z+Rk_y\hat{\sigma}_y+E_{e1X}^{\perp} \\ &\quad+\frac{J_\perp}{2}[1+\cos(k_z d)]+\frac{\hbar^2k_y^2}{2m_X^{\parallel}}+\frac{\hbar^2k_x^2}{2m_X^{\perp}} , \end{aligned} \tag{4.3}$$

$\hat{V}_{xy}$ is given by Eq. (3.4), and $E_{e1X}^{\perp}$ is the electron confinement energy in an AlAs quantum well.

In the absence of the X_x-X_y mixing, the low-lying-miniband solutions are

$$\Psi_{x\mathbf{k}}=\frac{e^{i\mathbf{k}_\perp\cdot\rho}}{\sqrt{\mathbf{S}}}\frac{1}{\sqrt{\mathbf{N}}}\sum_m e^{ik_z dm}u^0(z-md)\begin{bmatrix}\alpha(k_x)\\ \beta(k_x)\\ 0\\ 0\end{bmatrix}, \tag{4.4a}$$

$$\Psi_{y\mathbf{k}}=\frac{e^{i\mathbf{k}_\perp\cdot\rho}}{\sqrt{\mathbf{S}}}\frac{1}{\sqrt{\mathbf{N}}}\sum_m e^{i(k_z-c^*)dm}u^0(z-md)\begin{bmatrix}0\\ 0\\ \alpha(k_y)\\ \beta(k_y)\end{bmatrix}, \tag{4.4b}$$

$$\beta(k)=\left[\frac{1}{2}\left[1+\frac{\Delta/2}{[(\Delta/2)^2+R^2k^2]^{1/2}}\right]\right]^{1/2},$$
$$\alpha(k)=i(\mathrm{sgn}Rk)\left[\frac{1}{2}\left[1-\frac{\Delta/2}{[(\Delta/2)^2+R^2k^2]^{1/2}}\right]\right]^{1/2}, \tag{4.5}$$

$\mathbf{S}$ being the cross section of the structure in the (x,y) plane. The energies corresponding to the states $\Psi_{x\mathbf{k}}$ and $\Psi_{y\mathbf{k}}$ are

$$\begin{aligned}E_{x\mathbf{k}}&=E_{e1X}^{\perp}+\frac{J_\perp}{2}[1-\cos(k_z d)]+\frac{\hbar^2k_y^2}{2m_X^{\perp}}+\frac{\hbar^2k_x^2}{2m_X^{\parallel}}\\&\quad-[(\Delta/2)^2+R^2k_x^2]^{1/2},\\E_{y\mathbf{k}}&=E_{e1X}^{\perp}+\frac{J_\perp}{2}[1+\cos(k_z d)]+\frac{\hbar^2k_x^2}{2m_X^{\perp}}+\frac{\hbar^2k_y^2}{2m_X^{\parallel}}\\&\quad-[(\Delta/2)^2+R^2k_y^2]^{1/2}.\end{aligned} \tag{4.6}$$

The matrix element of the X_x-X_y mixing is obtained by using Eqs. (3.4), (4.4a), and (4.4b):

$$\begin{aligned}V_{xy}(\mathbf{k}_\perp)&\equiv\langle X_x,\mathbf{k}_\perp,k_z|\hat{V}_{xy}|X_y,\mathbf{k}_\perp,k_z-c^*\rangle\\&=V_{xy}^{(v)}\alpha^*(k_x)\alpha(k_y)+V_{xy}^{(u)}\beta^*(k_x)\beta(k_y),\end{aligned} \tag{4.7}$$

where

$$V_{xy}^{(u,v)}=2\cos(M\pi/2)a_0U^{(u,v)}[u^0(BA)]^2. \tag{4.8}$$

The mixed states X_{xy} are obtained by a replacement of the column in Eq. (4.4a) [or Eq. (4.4b)] by

$$\hat{F}^-=F_x\begin{bmatrix}\alpha(k_x)\\ \beta(k_x)\\ 0\\ 0\end{bmatrix}+F_y\begin{bmatrix}0\\ 0\\ \alpha(k_y)\\ \beta(k_y)\end{bmatrix} \tag{4.9a}$$

and

$$\hat{F}^+=-F_y\begin{bmatrix}\alpha(k_x)\\ \beta(k_x)\\ 0\\ 0\end{bmatrix}+F_x\begin{bmatrix}0\\ 0\\ \alpha(k_y)\\ \beta(k_y)\end{bmatrix} \tag{4.9b}$$

with

$$\begin{aligned}F_x&=\left[\frac{1}{2}\left[1+\frac{\Delta E/2}{[(\Delta E/2)^2+V_{xy}^2]^{1/2}}\right]\right]^{1/2},\\F_y&=\mathrm{sgn}V_{xy}\left[\frac{1}{2}\left[1-\frac{\Delta E/2}{[(\Delta E/2)^2+V_{xy}^2]^{1/2}}\right]\right]^{1/2},\end{aligned} \tag{4.10}$$

ΔE being the difference $E_{y\mathbf{k}}-E_{x\mathbf{k}}$. The corresponding energies are

$$E_{\mathbf{k}}^{\pm}=\bar{E}_{\mathbf{k}}\pm[(\Delta E/2)^2+V_{xy}^2]^{1/2}, \tag{4.11}$$

$$\begin{aligned}\bar{E}_{\mathbf{k}}&\equiv\frac{E_{x\mathbf{k}}+E_{y\mathbf{k}}}{2}=E_{e1X}^{\perp}\\&\quad+\frac{J_\perp}{2}+\tfrac{1}{4}\hbar^2k_\perp^2\left[\frac{1}{m_X^{\perp}}+\frac{1}{m_X^{\parallel}}\right]\\&\quad-\tfrac{1}{2}\{[(\Delta/2)^2+R^2k_x^2]^{1/2}+[(\Delta/2)^2+R^2k_y^2]^{1/2}\},\end{aligned} \tag{4.12}$$

$$\begin{aligned}\Delta E&\equiv E_{y\mathbf{k}}-E_{x\mathbf{k}}=J_\perp\cos(k_z d)\\&\quad+\tfrac{1}{2}\hbar^2(k_x^2-k_y^2)\left[\frac{1}{m_X^{\perp}}-\frac{1}{m_X^{\parallel}}\right]\\&\quad+[(\Delta/2)^2+R^2k_x^2]^{1/2}-[(\Delta/2)^2+R^2k_y^2]^{1/2},\end{aligned} \tag{4.13}$$

$k_\perp^2=k_x^2+k_y^2$. As expected the dispersion $E_{\mathbf{k}}^{\pm}$ is an invariant of the point group $D_{2d}\times i=D_{4h}$. Note: for the [110] and [1$\bar{1}$0] directions (with $k_x=\pm k_y$) the energy difference ΔE is equal to $J_\perp\cos(k_z d)$ and independent on $k_{x,y}$.

Figure 5 shows the electron energy structure for the lowest X_{xy} minibands calculated for the $(GaAs)_7(AlAs)_{10}$ SL. In order to obtain a better agreement with the numerical calculations by Lu and Sham,[3] we used the band parameters $\Delta_1=0.3$ eV, $m_X^{\perp,A}=0.30m_0$, and $m_X^{\perp,B}=0.23m_0$, the difference between the effective masses $m_X^{\perp}$ in the A and B layers being included in this calculation. Then the best-fit value for the X_x-X_y mixing coefficient $|t_{xy}^{(u)}|$ is close to 0.5. The similar comparison with the dispersion along [001] for the $(GaAs)_{11}(AlAs)_7$ SL (see Fig. 9 of Ref. 3) gives the Γ-X_z mixing coefficient $t_{\Gamma X}\approx 0.3$. We expect that the analytical results of the present work can be used to estimate both t_{xy} and $t_{\Gamma X}$ directly from experimental data.

B. Interminiband optical transitions

In this section we consider the light absorption in the $\mathbf{E}\perp z$ polarization for direct optical transitions between $E^-(\mathbf{k})$ and $E^+(\mathbf{k})$ minibands. To evaluate the absorption coefficient $\kappa(\omega)$, we use the standard formula

$$\begin{aligned}\kappa(\omega)=\frac{4\pi^2e^2}{\omega c(\varepsilon_b)^{1/2}}\frac{2}{V}\sum_{\mathbf{k}}&|\langle+,\mathbf{k}|\mathbf{e}\cdot\hat{\mathbf{v}}|-,\mathbf{k}\rangle|^2\\&\times[f(E_{\mathbf{k}}^-)-f(E_{\mathbf{k}}^+)]\\&\times\delta(E_{\mathbf{k}}^+-E_{\mathbf{k}}^--\hbar\omega),\end{aligned} \tag{4.14}$$

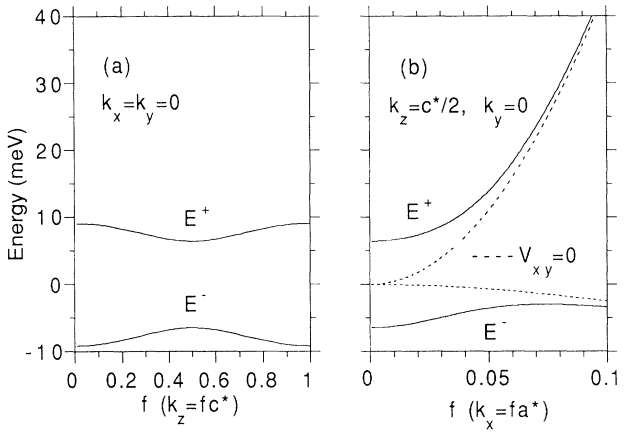

FIG. 5. Electron minibands X_{xy} in the ideal $(GaAs)_7(AlAs)_{10}$ SL along $(a^*,0,fc^*)$ (a) and $(a^*+fa^*,0,c^*/2)$ (b). k_x and k_y are referred to the X_x point $(a^*,0,0)$. The dispersion (a) agrees with that for the lowest-lying minibands calculated by Lu and Sham using a second-neighbor tight-binding method and shown in Fig. 10(c) of Ref. 3.

where ω is the frequency and $\mathbf{e}$ is the polarization unit vector of the light wave, $\hat{\mathbf{v}}$ is the electron velocity operator, ε_b is the background dielectric constant, $f(E)$ is the electron energy distribution function, the factor 2 accounts for the spin state degeneracy, and V is the SL sample volume. In the representation (4.1) the transverse velocity operator is given by

$$\hat{v}_x=\frac{1}{\hbar}\frac{\partial H}{\partial k_x}=\begin{bmatrix}(R/\hbar)\hat{\sigma}_y & 0\\ 0 & \hbar k_x/m_X^{\perp}\end{bmatrix},$$
$$\hat{v}_y=\frac{1}{\hbar}\frac{\partial H}{\partial k_y}=\begin{bmatrix}\hbar k_y/m_X^{\perp} & 0\\ 0 & (R/\hbar)\hat{\sigma}_y\end{bmatrix}. \tag{4.15}$$

Using Eqs. (4.9) and (4.15) one can derive the following expressions for the interminiband matrix elements:

$$v_\gamma(\mathbf{k})\equiv\langle +,\mathbf{k}|\hat{v}_x|-,\mathbf{k}\rangle = \pm F_xF_y\left[\frac{\hbar k_\gamma}{m_X^{\perp}}-2i\alpha(k_\gamma)\beta(k_\gamma)\frac{R}{\hbar}\right], \tag{4.16}$$

where the right-hand side $\pm$ corresponds to $\gamma=x$ and y, respectively. Taking into account that

$$-2i\alpha(k)\beta(k)=\frac{Rk}{[(\Delta/2)^2+R^2k^2]^{1/2}} \tag{4.17}$$

and

$$F_xF_y=\frac{1}{2}\frac{V_{xy}}{[(\Delta E/2)^2+V_{xy}^2]^{1/2}}=\frac{V_{xy}}{\hbar\omega}, \tag{4.18}$$

we can rewrite Eq. (4.16) in the form

$$v_\gamma(\mathbf{k})=\pm\frac{V_{xy}}{\hbar\omega}\frac{\hbar k_\gamma}{m_X^{\perp}}\left[1+\frac{m_X^{\perp}R^2}{\hbar^2[(\Delta/2)^2+R^2k_\gamma^2]^{1/2}}\right]. \tag{4.19}$$

Note that for AlAs band parameters the second term in the brackets is small as compared with unity, and for simplicity in the following this term is omitted. Since the absorption coefficient is independent on the polarization direction in the (x,y) plane, the matrix-element squared modulus in Eq. (4.14) can be replaced by

$$\tfrac{1}{2}[v_x^2(\mathbf{k})+v_y^2(\mathbf{k})].$$

Further simplifications can be achieved by neglecting the electron dispersion along k_z, so that the sum over k_z in Eq. (4.14) can be replaced by the inverse period, d^{-1}, and by using the approximations

$$\bar{E}_{\mathbf{k}}\approx E_{e1X}^{\perp}-\frac{\Delta}{2}+\frac{\hbar^2k_{\perp}^2}{4m_X^{\perp}},$$
$$\Delta E\approx\frac{\hbar^2(k_x^2-k_y^2)}{2m_X^{\perp}}, \tag{4.20}$$
$$V_{xy}(\mathbf{k})\approx V_{xy}^{(u)},$$

which are valid if $\hbar\omega-\Delta_{xy}\ll\Delta$, Δ_{xy} being the miniband splitting $2|V_{xy}^{(u)}|$ at the X point (Fig. 5). Define

$$p=\frac{[(\hbar\omega)^2-\Delta_{xy}^2]^{1/2}}{2k_BT},\quad J(p)=\int_0^\infty dx\,e^{-x}\frac{x+p}{\sqrt{x(x+2p)}},$$

then we obtain

$$\kappa(\omega)=\frac{4e^2}{dc\hbar(\varepsilon_b)^{1/2}}\left[\frac{\Delta_{xy}}{\hbar\omega}\right]^2 sh\left[\frac{\hbar\omega}{2k_BT}\right]e^{\mu/k_BT}\frac{e^{-p}}{p}J(p), \tag{4.21}$$

where the Boltzmann distribution is used for the X electrons and k_B is the Boltzmann constant. The chemical potential μ is calculated from the electron density in the X_{xy} states:

$$n_{xy}=2e^{\mu/k_BT}\sum_{\mathbf{k},\pm}\exp[-(E_{\mathbf{k}}^{\pm}+\Delta/2-E_{1eX}^{\perp})/k_BT]. \tag{4.22}$$

For frequencies ω close to the absorption edge $\omega_{xy}=\Delta_{xy}/\hbar$ one can use the following crude estimation:

$$\kappa(\omega)\approx 2\pi\frac{e^2}{c\hbar(\varepsilon_b)^{1/2}}\frac{\hbar^2n_{xy}^{(2D)}}{k_BTd(m_X^{\perp}m_X^{\parallel})^{1/2}}, \tag{4.23}$$

where $n_{xy}^{(2D)}=dn_{xy}$, n_{xy} being the three-dimensional density (4.22). Recall that the relative positions of X_z and X_{xy} valleys in type-II GaAs/AlAs SL's were analyzed by Scalbert *et al.*[17] For $T=100$ K, $d=50$ Å, Eq. (4.23) gives $\kappa(\omega)\approx 40(n_{xy}^{(2D)}/n_0)$ (cm^{-1}), the reference density n_0 being 10^{10} cm^{-2}. It should be stressed that, in the absence of X_x-X_y mixing, direct optical intraband transitions in n-type SL's are forbidden in the $\mathbf{E}\perp z$ polarization.

V. CONCLUSION

It should be mentioned that for ultrashort-period SL's like 2×2 or 3×3 SL's, the proposed effective-mass ap-

proximation can be invalid and gives only a qualitative description. In this case first-principle calculations are necessary.

In conclusion, the version of the effective-mass approximation proposed in this work can be readily and successfully extended to treat valley mixings in multilayer GaAs/AlAs structures grown along other high-symmetry axes, say along [110] or [111], and in structures with other compositional materials.

ACKNOWLEDGMENT

The work was partially supported by the Swedish Research Council for Engineering Sciences.

[1]E. E. Mendez, E. Calleja, C. E. T. Goncalves da Silva, L. L. Chang, and W. I. Wang, Phys. Rev. B **33**, 7368 (1986).
[2]M.-H. Meynadier, R. E. Nahory, J. M. Worlock, M. C. Tamargo, J. L. de Miguel, and M. D. Sturge, Phys. Rev. Lett. **60**, 1338 (1988).
[3]Y.-T. Lu and L. J. Sham, Phys. Rev. B **40**, 5567 (1989).
[4]I. Morrison, L. D. L. Brown, and M. Jaros, Phys. Rev. B **42**, 11 818 (1990).
[5]L. J. Sham and Y.-T. Lu, J. Lumin. **44**, 207 (1989).
[6]H. Kamimura and T. Nakayama, in *Proceedings of the 18th International Conference on the Physics of Semiconductors, Stockholm, 1986,* edited by O. Engström (World Scientific, Singapore, 1987), Vol. 1, p. 643.
[7]J. Ihm, Appl. Phys. Lett. **50**, 1068 (1987).
[8]M. A. Gell, D. Ninno, M. Jaros, D. J. Wolford, T. F. Keuch, and J. A. Bradley, Phys. Rev. B **35**, 1196 (1987).
[9]D.Z.-Y. Ting and Y.-C. Chang, Phys. Rev. B **36**, 4359 (1987).
[10]Y. I. Polygalov and A. S. Poplavnoi, Fiz. Tekh. Poluprovodn. **24**, 328 (1990) [Sov. Phys. Semicond. **24**, 201 (1990)].
[11]J.-B. Xia and Y.-C. Chang, Phys. Rev. B **42**, 1781 (1990).
[12]T. Ando and H. Akera, Phys. Rev. B **40**, 11 619 (1989).
[13]J.-B. Xia, Phys. Rev. B **41**, 3117 (1990).
[14]H. C. Liu, Superlatt. Microstruct. **7**, 35 (1990).
[15]I. A. Aleiner and E. L. Ivchenko, Fiz. Tekh. Poluprovodn. **27**, 594 (1993) [Sov. Phys. Semicond. (to be published)].
[16]G. Danan, B. Etienne, F. Mollot, R. Planel, A. M. Jean-Louis, F. Alexandre, B. Jusserand, G. Le Roux, J. Y. Marzin, H. Savary, and B. Sermage, Phys. Rev. B **35**, 6207 (1987).
[17]D. Scalbert, J. Cernogora, C. Benoit à la Guillaume, M. Maaref, F. F. Charfi, and R. Planel, Solid State Commun. **70**, 945 (1989).
[18]O. Madelung, W. von der Osten, and U. Rössler, in *Intrinsic Properties of Group IV Elements and III-V, II-VI and I-VII Compounds,* edited by O. Madelung, Landolt-Börnstein, New Series, Group III, Vol. 22, Pt. a (Springer-Verlag, Berlin, 1987).